Atmospheric Research 138 (2014) 278–292

Contents lists available at ScienceDirect

Atmospheric Research

journal homepage: www.elsevier.com/locate/atmos

Size fractionated aerosol composition at roadside and background environments in the Madrid urban atmosphere

Fátima Mirante [a,*], Pedro Salvador [b], Casimiro Pio [a], Célia Alves [a], Begoña Artiñano [b], Alexandre Caseiro [a], M[a]. Aranzazu Revuelta [b]

[a] CESAM, Department of Environment and Planning, University of Aveiro, Campus de Santiago, 3810-193 Aveiro, Portugal
[b] CIEMAT, Atmospheric Pollution Unit, Environmental Department, Av. Complutense 22, 28040 Madrid, Spain

ARTICLE INFO

Article history:
Received 7 June 2013
Received in revised form 13 October 2013
Accepted 25 November 2013

Keywords:
Mass size distribution
Chemical speciation
Ionic components
Minerals
Organic carbon
Urban aerosols

ABSTRACT

The chemical composition of size-segregated particulate matter (PM) was studied during summer and winter sampling campaigns, at two different urban sites (roadside and urban background) in the city of Madrid, Spain. PM was sampled with high volume cascade impactors, in 4 size ranges: 10–2.5, 2.5–1, 1–0.5 and <0.5 μm. The carbonaceous content (OC and EC) was determined by a thermo-optical method, whilst the water soluble ionic species were measured by ion chromatography. The most common synoptic meteorological situations, including those causing the transport of African dusty air masses, were identified in both seasons. Whether the PM_{10} mass or the highest concentrations of EC and OC were found predominantly in the ultrafine size fraction at both sites. In contrast with roadside, at the urban background, the particle mass concentrations for the different size ranges were statistically higher in summer than in winter. Observed inter-site differences suggest the existence of other sources and formation processes contributing in the summer period to the levels of PM at the urban background site apart from road traffic emissions. Secondary organic carbon (SOC) showed a clear seasonal pattern, with much higher concentrations in summer than in winter in both places, as well as higher relative contributions at the urban background than at the road traffic site. $(NH_4)_2SO_4$ levels were at their maximum at both sites in summer in $PM_{0.5}$. Differently, higher values were reached in winter for NH_4NO_3 in $PM_{0.5}$ and for NaCl in $PM_{2.5–10}$. From the ion balances, it was observed that, in summer, the formation of secondary inorganic compounds included an unusual enrichment in Ca^{2+} in the submicrometre fraction, either at roadside or at urban background.

1. Introduction

Particulate matter (PM) is a high priority atmospheric pollutant since it has strong negative impacts on human health, (Schleicher et al., 2011), climate (Das and Jayaraman, 2012), acid rain (Zhang et al., 2012), ecosystems (Katul et al., 2011), visibility (Yuan et al., 2006) and building materials (Costa et al., 2009).

A major portion of atmospheric particles is constituted by carbonaceous matter (elemental (EC), organic carbon (OC), carbonated carbon (CC)); at European urban areas, its contribution is known to reach up to 18–32% of PM_{10} and 25–31% of $PM_{2.5}$ (Putaud et al., 2010). Epidemiological studies have demonstrated that cardiovascular mortality and morbidity are associated with exposure to increased levels of urban carbonaceous aerosols (Ito et al., 2011). EC is abundant in the emissions from combustion of fossil fuel (Gillies and Gertler, 2000), and biomass burning (Alves et al., 2010; Vicente et al., 2012). OC sources are poorly characterised, but include direct emission by combustion processes, soil, paved road dust, meat cooking and others, and gas to particle conversion from anthropogenic and biogenic volatile organic compounds (VOCs). OC and EC are two of the major components of atmospheric particles emitted by traffic (both diesel and gasoline) (Calvo et al., 2013). There is little information

* Corresponding author. Tel.: +351 234 370 958; fax: +351 234 370 309.
E-mail address: fmirante@ua.pt (F. Mirante).

0169-8095/$ – see front matter © 2013 Elsevier B.V. All rights reserved.
http://dx.doi.org/10.1016/j.atmosres.2013.11.024

concerning the loading of CC in aerosols in Europe; CC results from soil or road dust emission and is usually present in coarse particles not attacked by atmospheric acidic components (Calvo et al., 2013).

Another predominant fraction of atmospheric aerosols consists in water soluble inorganic matter (WSIM). WSIM is emitted directly in the particulate form, principally as sea salt from the action of wind on the ocean surface (Donahue et al., 2009) or as secondary production from gas to particle conversion. Sulphate, nitrate and ammonia are considered the major secondary inorganic compounds in aerosols; their precursor gases (SO_2, NO_x and NH_3) are mainly emitted to the atmosphere by combustion processes (energy production or road traffic) and agricultural activities. At European urban areas, sulphate and nitrate contributions are known to reach up to 21–28% of PM_{10} and 22–37% of $PM_{2.5}$ (Putaud et al., 2010).

Given that the presently in-force European Directive 2008/50/EC on air quality, requires the control of PM_{10} and $PM_{2.5}$, many studies have been focussed on the size integrated particulate matter, mainly in urban areas (Aldabe et al., 2011; Minguillón et al., 2012; Moreno et al., 2013; Oliveira et al., 2010; Salvador et al., 2012). However, the environmental effects, the formation processes and the source assignment depend greatly on the particle size distribution (Lighty et al., 2000). Concerning size-segregated samples, attention has been greatly focussed on polyaromatic hydrocarbons in urban areas, because of their carcinogenicity (Cancio et al., 2004; Duan et al., 2005; Wang et al., 2009). The information available on the particle size distributions for other compounds is rather scarce.

The Madrid metropolitan area is located in the central part of the Iberian Peninsula, where extreme weather conditions associated with an inland climate are usual. The region has no relevant nearby heavy industrial activity, being the traffic sector the dominant emission source of carbonaceous matter (Salvador et al., 2004, 2012). Moreover, residential wood burning activities are rather inexistent in this urban area. Domestic heating devices in Madrid City in 2009–2010 were preferably fed by natural gas (74%), fuel-oil (19%), coal (4%), butane (2%) and propane (1%) (Ayuntamiento, 2010). Over the last years atmospheric pollution levels have been decreasing in the metropolitan area due to a reduction in residential coal burning emissions and to changes in the vehicle fleet composition (Salvador et al., 2012). However, long-range transport episodes of mineral dust, usually related to the occurrence of African dust outbreaks, significantly affect aerosol concentrations in the Madrid air basin (Salvador et al., 2004). The concentration of inhalable mineral dust in Madrid air is also strongly influenced by traffic resuspension (Moreno et al., 2013).

This study reports, for the first time, data from four size fractions in two distinct places in the metropolitan area of Madrid (Spain), one with fresh traffic influence and the other in a suburban area, for two periods of time during the summer of 2009 and the winter of 2010. The innovative character of this study consists in obtaining time series with a size-segregated detailed chemical composition of PM for differently polluted urban sites, which may be further used for a more accurate assessment of emission sources and atmospheric processes (Lighty et al., 2000). It would be important to understand how the above mentioned components behave in the small size fractions, helping to fulfil the task of reducing human exposure to PM.

2. Methods

2.1. Sampling site

The Madrid metropolitan area is located in the Madrid air basin, at the centre of the Iberian Peninsula. This basin is bordered to the north–northwest by the Sierra de Guadarrama range, located 40 km from the metropolitan area, to the northeast–east by lower mountainous terrain and to the South by the Toledo Mountains (Fig. 1). Population is about 6.6 million inhabitants, involving a car fleet of almost 4 million vehicles with very intense traffic on weekdays on the two existing ring roads and the roads connecting Madrid with the surrounding towns, where more than 2.5 million residents live (Gómez-Moreno et al., 2007).

One sampling site was located next to an automatic monitoring station (Escuelas Aguirre) which belongs to the Madrid municipality Air Quality Network. It is located at a heavy traffic street intersection in Madrid downtown (Fig. 1). The distance to the kerbside was approximately 5 m. Escuelas Aguirre provides a classical example of a city centre roadside traffic polluted site, dominated by the daily double peak in PM, NO_x, and CO concentrations, associated with morning and evening journeys across the city (Moreno et al., 2013).

The other sampling point was positioned within a non-residential, non-traffic area on the NW outskirts of Madrid (CIEMAT, Fig. 1). It is located downwind of the city centre, between the main university campus, “Ciudad Universitaria” and “La Dehesa de la Villa” park. The nearest road (Complutense Avenue) is separated from the site by more than 300 m and no industrial or domestic heating sources are present in the vicinity. Thus, according to the criteria established by the E.E.A. (European Environment Agency) (1999) this station can be classified as an urban background site. From now on, the Escuelas Aguirre traffic site and the CIEMAT urban background site will be designated as EA and CIE, respectively.

2.2. Sampling

Sampling campaigns were carried out in June of 2009 and January–February of 2010. About 30 days of sampling was done for each summer and winter campaigns. Samples were collected in parallel at both sites during 24 h, starting at 08:00–09:00, local time. High volume samplers, operating at a flow of 1.13 $m^3\ min^{-1}$, were equipped with a PM_{10} size selective inlet and a cascade impactor, from Tisch Environmental, Inc., which consists in three stages and a back-up filter (20.3 × 25.4 cm). Particles were collected in four size fractions: <0.49, 0.49–0.95, 0.95–2.5, and 2.5–10 μm. For easiness, cutting size values will be expressed throughout the paper, in an approximated way, as <0.5, 0.5–1, 1–2.5, and 2.5–10 μm. For comparison with the standard parameters more frequently used in air quality requirements, concentration values are also reported as PM_1, $PM_{2.5}$ and PM_{10}.

Particle matter collection was carried out onto quartz fibre filters from Whatman (QM-A) pre-fired (500 °C for 6 h). At the EA site NO_2, NO_x and CO hourly concentration levels were obtained from the local automatic station. At the CIE site, gaseous species NO, NO_2 and O_3 were measured using a calibrated DOAS spectrometer (OPSIS, model AR-500) along a

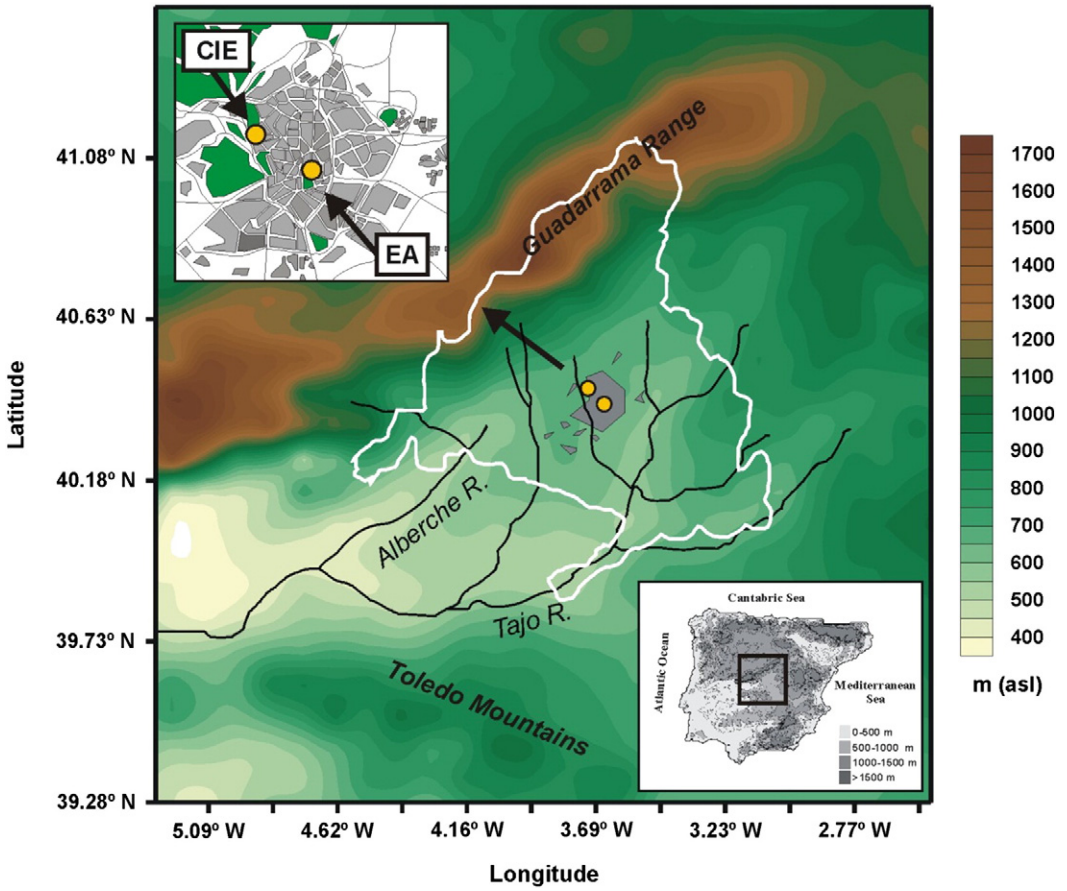

Fig. 1. Bi-dimensional topography of the Madrid Air Basin, located in the centre of the Iberian Peninsula (down-right). The locations of the EA and CIE monitoring sites are shown. The metropolitan area, represented by the city of Madrid (up-left) and satellite towns, has been shaded. White line represents the boundary of the Madrid province territory.

228 m horizontal path with a mean height of 10 m above ground located next to the PM sampler.

2.3. Analytical methodologies

Before sampling, the filters were pre-conditioned in a chamber with controlled ambient conditions with constant humidity (50 ± 5%) and temperature (20 ± 1 °C) for a minimum period of 24 h, and then weighted. After collection, the filters were re-conditioned, re-weighed and temporarily stored in a freezer (−20 °C) until analysis.

The EC and OC carbon fractions were analysed by a home-made thermo-optical transmission system described in detail elsewhere (Pio et al., 2011), using a protocol similar to EUSAAR. Coarse fraction samples were decarbonated with HCl fumes, previously to OC/EC analysis. The accuracy of this method for measuring the total carbon content was regularly ascertained by analysing a known quantity of potassium hydrogen phthalate applied to blank quartz fibre filters. Relative standard deviations are less than 3%. Precision, measured as a relative standard deviation from replicate analyses of the same samples, fell in the 4–6% range. The uncertainties were estimated from the coefficient of variance for replicate analysis and from the minimum detection limits (Chow et al., 2005). Detection limits depend mainly on the variability of filter blanks (adsorption of volatile organic compounds during storage and transport) and the noises of both the laser and the CO_2 analyser. On the basis of the variability of blank filter batches, the detection limit of OC (3 times the standard deviation) was found to be of the order of 30–80 ng m^{-3}. Evaluation of thermograms shows that masses of carbon lower than 1 μg are difficult to quantify, with the applied methodology, for low filter particle deposits. That corresponds to a detection limit of 30 ng m^{-3} for EC. Overall, the uncertainty was found to be less than ±12%. The methodology used in this study was tested with the NIST (National Institute of Standards and Technology) filter standard and in an intercomparison experiment with real aerosol samples (Schmid et al., 2001), delivering OC/EC ratios between those obtained by the NIOSH (National Institute for Occupational Safety and Health) and the IMPROVE (Interagency Monitoring of Protected Visual Environments) protocols, but closer to the latter. The procedure was also compared with the EUSAAR (European Supersites for Atmospheric Aerosol Research) II protocol through the analysis of samples of different types and origins and the results proved to be similar (Almeida, 2009).

Carbonates were analysed through the release of CO_2, and measured by the same non-dispersive infrared analyser coupled to the thermo-optical system, when a punch of each filter was acidified with orthophosphoric acid (20%) in a free CO_2 gas stream. After a screening of representative

samples from different time periods and covering all the particle size ranges, it was found that only the coarsest fractions contained quantifiable masses of carbonates. Thus, an exhaustive determination of CC was carried out only in $PM_{1-2.5}$ and $PM_{2.5-10}$ size ranges.

For the determination of water soluble inorganic ions, one filter strip from the $PM_{2.5-10}$, $PM_{2.5-1}$ and $PM_{1-0.5}$ (11 cm^2) slotted filters and 4 punches of 1.3 cm diameter (5.3 cm^2) from the 398 cm^2 sampled area of the $PM_{0.5}$ were extracted with ultra-pure water with resistivity lower than 18.2 MΩ cm. Ion chromatography, using Dionex AS14 and CS12 chromatographic columns, with Dionex AG14 and CG12 guard columns, coupled to Dionex AMMS II and Dionex CMMS III suppressors, and to Dionex DX-100 and Shimadzu CDD-6A detectors, was employed to analyse anions (Cl^-, NO_3^- and SO_4^{2-}) and cations (Na^+, NH_4^+, K^+, Mg^{2+} and Ca^{2+}), respectively.

2.4. Meteorological analysis

A determination of the dominant synoptic meteorological situations over the study area was carried out by analysis of meteorological charts and atmospheric back-trajectories. Five-day 3D backward air trajectories were computed using the HYSPLIT model and GDAS meteorological data sets (Draxler and Rolph, 2003). Back-trajectories were generated at 00:00, 06:00, 12:00 and 18:00 h UTC for any day of the study periods, with origin over both sampling sites at 750, 1500 and 2500 m above ground level (AGL). Specific synoptic meteorological situations were determined and represented with meteorological variables from the NOAA/OAR/ESRL PSD-USA NCEP/NCAR Reanalysis dataset files (Kalnay et al., 1996).

The occurrence of African dust outbreaks over this area was documented on the basis of this meteorological analysis and information obtained from satellite imagery and numerical models. The methodology described by Salvador et al. (2013) to detect African dust outbreaks reaching the Madrid Air Basin was used.

Complementarily, local meteorological information was obtained from an instrumented tower permanently installed at CIEMAT which provided wind speed, wind direction and temperature data at 80 m and temperature, relative humidity and dew point data at 10 m height.

3. Results and discussion

3.1. Meteorological conditions

Atmospheric conditions were rather variable during both sampling periods. As a consequence PM levels (Fig. 2) were influenced by the concatenation of the different events.

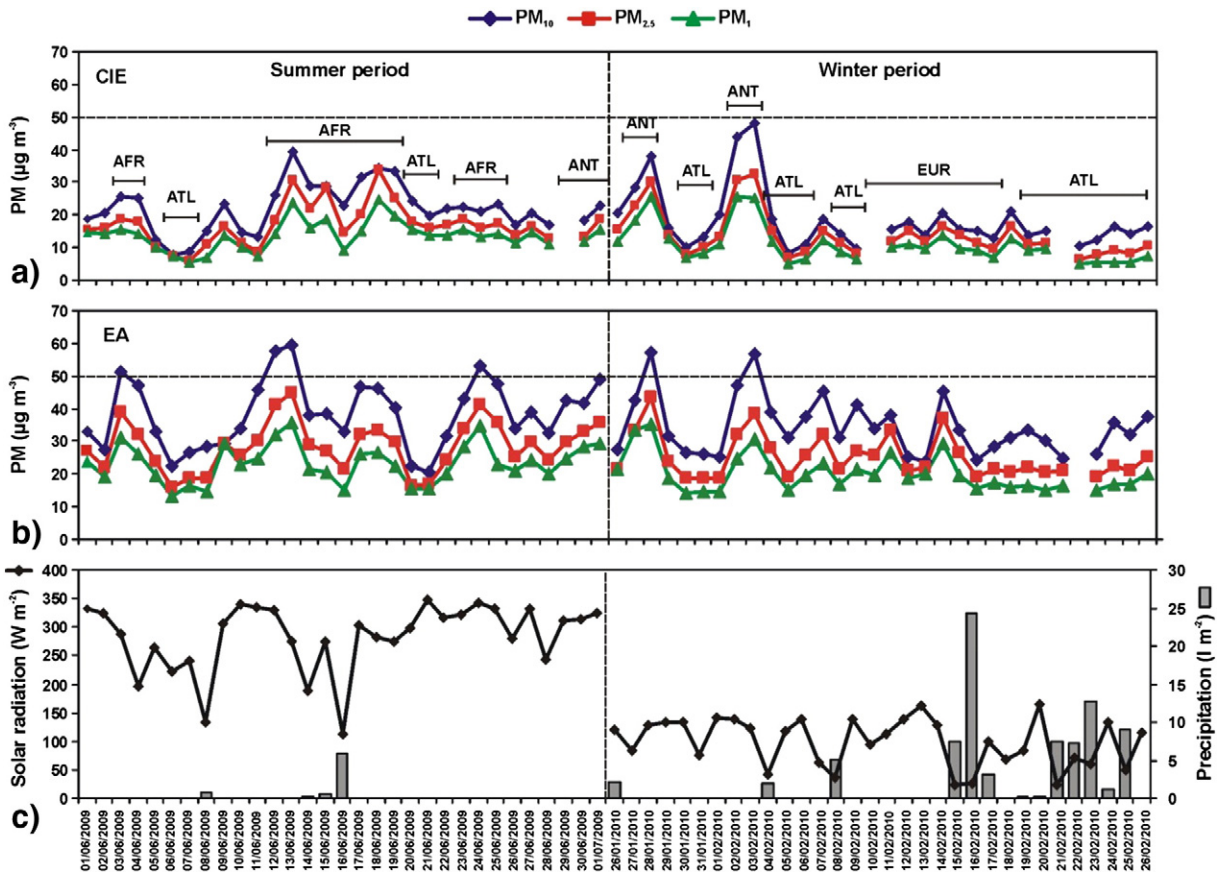

Fig. 2. PM daily concentration levels registered at CIE (a) and EA (b) sites during June 2009 (summer period) and January–February 2010 (winter period). Daily mean solar radiation and daily accumulated precipitation levels, registered at CIE (c). Specific events are highlighted (AFR—African dust outbreak; ATL—Atlantic advection; ANT—Local pollution episode; EUR—European air masses advection).

Illustrative synoptic meteorological situations causing these events are represented by composite sea level pressure or geopotential height maps (Fig. 3).

The synoptic meteorological situation during the summer sampling period was dominated by the advection of African air mass (AFR) towards the Iberian Peninsula (Fig. 3a). Three African dust outbreaks were identified, in the periods 3–4 June, 12–19 June and 23–25 June 2009, influencing PM levels in the Madrid Air Basin, especially in the first two events. The advection of Atlantic air masses (ATL) between 6 and 8 June 2009 and 20–21 June 2009, resulted in the lower PM levels registered in this period at both sampling sites.

During more than 50% of the winter period days, clean air masses associated with the passage of Atlantic frontal systems, were continuously transported to the Madrid Air Basin (Fig. 3b). Additionally, air masses coming from the European continent (EUR) were also identified between 10 and 14 February 2010 (Fig. 3c). This synoptic meteorological situation gave rise to an intense cold wave over the central area of the Iberian Peninsula, generating precipitation as rain and snow (Fig. 2c).

During sampling only short periods were characterised by stable anticyclone stagnation conditions (ANT) (development of intensive thermal inversions, lower convective dynamics and low dispersive local circulations); this synoptic situation (Fig. 3d) favours the accumulation of pollutants near the emission sources, frequently giving rise to local pollution episodes in the Madrid urban area (Artiñano et al., 2003). These episodes took place in the periods 29 June–01 July 2009, 28–29 January 2010 and 2–3 February 2010.

3.2. PM levels

A summary of aerosol concentrations and composition is given in Table 1. Mean PM_{10} concentration levels were 38 and 21 μg m^{-3} in summer and 34 and 18 μg m^{-3} in winter at, respectively, EA and CIE sites. The $PM_{2.5–10}$, $PM_{1–2.5}$, $PM_{0.5–1}$ and $PM_{0.5}$ contributions to PM_{10} were estimated to be 26, 13, 8 and 54%, respectively, at the EA site in summer and 25, 16, 13 and 47% in winter. At the CIE site, these contributions were very similar for both seasons (24, 13, 8 and 55% in summer and 25, 16, 13 and 47% in winter). Thus, the PM_{10} mass was found predominantly in the ultrafine fraction (Dp < 0.5) and, to a lesser extent, in the coarse (Dp > 2.5–10) fraction. The contribution to the PM_{10} mass from both fractions increased during summertime (Table 1).

The Mann–Whitney test was applied to assess seasonal differences in each sampling site. This is a non-parametric statistical hypothesis test for assessing whether one of two

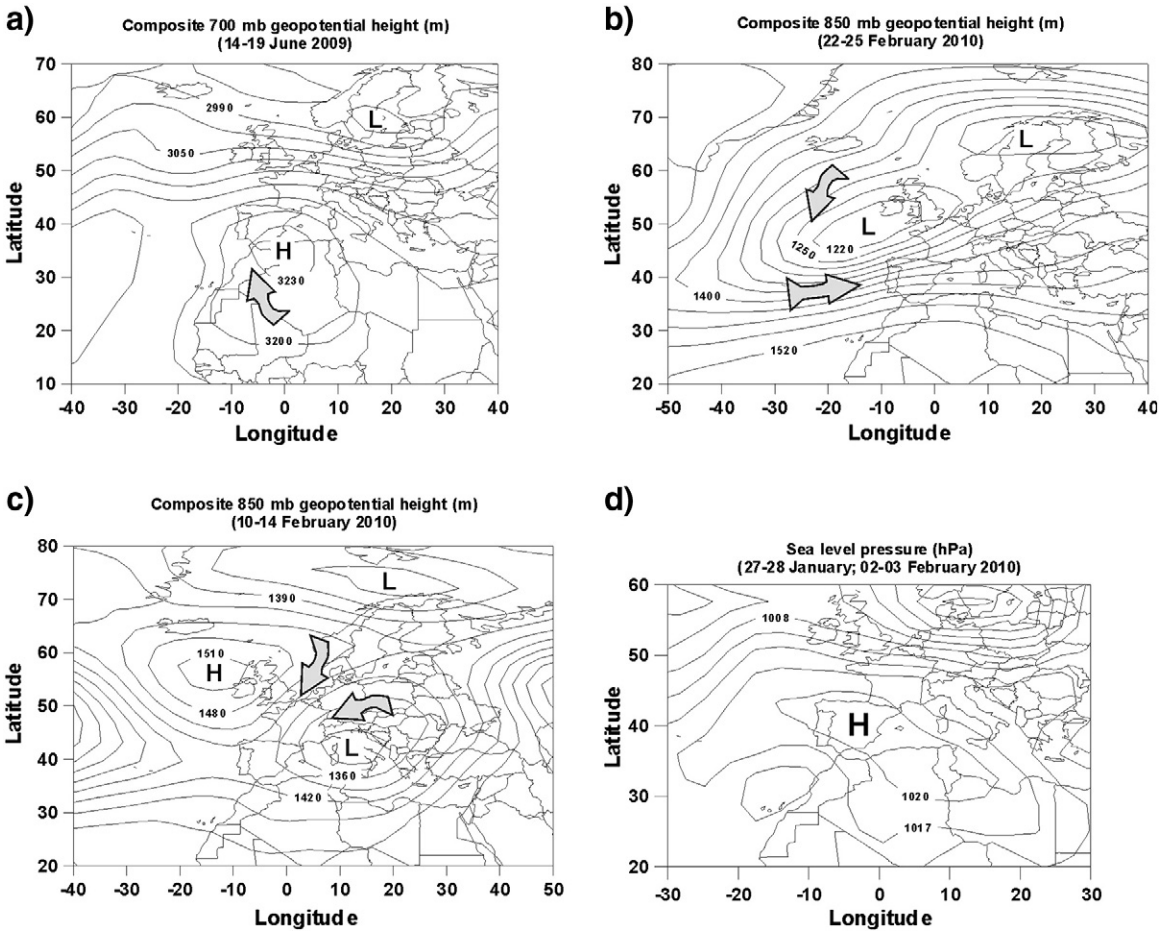

Fig. 3. Composite sea level pressure (hPa), 850 or 700 mb geopotential height (m) maps, during specific events (African (a), Atlantic (b) and European (c) air mass advections and anticyclone stagnation conditions (d)).

Table 1
Mean concentration values and standard deviation (C ± SD) in μg m^{-3} of each chemical species by size at the roadside and urban background in summer and winter.

	Roadside				Urban Background			
	$PM_{2.5-10}$	$PM_{1-2.5}$	$PM_{0.5-1}$	$PM_{0.5}$	$PM_{2.5-10}$	$PM_{1-2.5}$	$PM_{0.5-1}$	$PM_{0.5}$
Summer								
Total mass	10 ± 2.7	5.3 ± 1.8	3.0 ± 0.91	21 ± 4.5	5.2 ± 1.5	2.9 ± 0.97	1.7 ± 0.74	12 ± 2.4
OC	0.75 ± 0.18	0.62 ± 0.15	0.77 ± 0.24	3.1 ± 0.66	0.52 ± 0.29	0.40 ± 0.10	0.41 ± 0.10	1.9 ± 0.45
EC	0.46 ± 0.13	0.34 ± 0.11	0.37 ± 0.17	3.1 ± 0.95	0.15 ± 0.083	0.095 ± 0.032	0.12 ± 0.049	0.72 ± 0.24
CO_3^{2-}	0.30 ± 0.17	0.15 ± 0.12	–	–	0.29 ± 0.33	0.10 ± 0.078	–	–
Cl^-	0.08 ± 0.08	0.03 ± 0.02	0.01 ± 0.005	0.1 ± 0.03	0.03 ± 0.04	0.02 ± 0.01	0.01 ± 0.01	0.13 ± 0.034
NO_3^-	0.31 ± 0.16	0.21 ± 0.065	0.083 ± 0.019	0.38 ± 0.10	0.29 ± 0.17	0.17 ± 0.052	0.077 ± 0.033	0.44 ± 0.12
SO_4^{2-}	0.16 ± 0.045	0.18 ± 0.064	0.28 ± 0.10	0.71 ± 0.18	0.11 ± 0.037	0.13 ± 0.052	0.22 ± 0.087	0.67 ± 0.20
Na^+	0.09 ± 0.05	0.07 ± 0.03	0.03 ± 0.02	0.02 ± 0.07	0.1 ± 0.08	0.08 ± 0.04	0.02 ± 0.01	0.1 ± 0.06
NH_4^+	0.003 ± 0.001	0.01 ± 0.006	0.06 ± 0.02	0.2 ± 0.05	0.003 ± 0.002	0.01 ± 0.01	0.06 ± 0.02	0.2 ± 0.07
K^+	0.02 ± 0.005	0.01 ± 0.03	0.01 ± 0.005	0.03 ± 0.01	0.01 ± 0.01	0.01 ± 0.01	0.01 ± 0.02	0.03 ± 0.04
Mg^{2+}	0.01 ± 0.004	0.01 ± 0.03	0.01 ± 0.002	0.01 ± 0.04	0.01 ± 0.01	0.01 ± 0.004	0.01 ± 0.002	0.01 ± 0.004
Ca^{2+}	0.1 ± 0.04	0.08 ± 0.02	0.08 ± 0.002	0.2 ± 0.06	0.08 ± 0.04	0.05 ± 0.02	0.06 ± 0.03	0.1 ± 0.04
Winter								
Total mass	9.2 ± 3.7	5.4 ± 1.6	4.1 ± 1.8	16 ± 4.8	4.5 ± 3.2	2.9 ± 1.3	2.3 ± 1.4	8.6 ± 4.8
OC	0.64 ± 0.57	0.69 ± 0.38	0.79 ± 0.34	1.8 ± 0.92	0.21 ± 0.24	0.20 ± 0.22	0.39 ± 0.34	0.61 ± 0.60
EC	0.42 ± 0.24	0.57 ± 0.28	0.46 ± 0.23	3.0 ± 0.90	0.11 ± 0.082	0.26 ± 0.091	0.17 ± 0.13	1.1 ± 0.96
CO_3^{2-}	0.21 ± 0.34	n.d.	–	–	0.22 ± 0.124	–	–	–
Cl^-	0.51 ± 0.34	0.20 ± 0.20	0.056 ± 0.059	0.10 ± 0.14	0.28 ± 0.24	0.097 ± 0.086	0.028 ± 0.032	0.025 ± 0.038
NO_3^-	0.16 ± 0.13	0.36 ± 0.25	0.34 ± 0.29	0.72 ± 0.56	0.12 ± 0.10	0.30 ± 0.21	0.31 ± 0.32	0.55 ± 0.60
SO_4^{2-}	0.16 ± 0.073	0.19 ± 0.10	0.19 ± 0.14	0.41 ± 0.21	0.073 ± 0.052	0.14 ± 0.11	0.18 ± 0.14	0.29 ± 0.16
Na^+	0.28 ± 0.23	0.15 ± 0.10	0.047 ± 0.044	0.087 ± 0.11	0.20 ± 0.15	0.094 ± 0.064	0.034 ± 0.017	0.04 ± 0.04
NH_4^+	0.003 ± 0.003	0.09 ± 0.09	0.1 ± 0.1	0.4 ± 0.2	0.003 ± 0.002	0.08 ± 0.08	0.1 ± 0.1	0.3 ± 0.2
K^+	0.01 ± 0.008	0.02 ± 0.01	0.01 ± 0.005	0.03 ± 0.02	0.008 ± 0.07	0.01 ± 0.008	0.02 ± 0.02	0.02 ± 0.02
Mg^{2+}	0.02 ± 0.01	0.01 ± 0.009	0.01 ± 0.002	0.01 ± 0.002	0.01 ± 0.02	0.009 ± 0.007	0.003 ± 0.002	0.001 ± 0.002
Ca^{2+}	0.1 ± 0.06	0.1 ± 0.05	0.08 ± 0.002	0.09 ± 0.06	0.05 ± 0.04	0.04 ± 0.03	0.03 ± 0.02	0.03 ± 0.04

n.d.—not detected.

samples of independent observations tends to have larger values than the other. At EA there was no statistically seasonal significant difference for PM_{10}, $PM_{2.5}$ and PM_1 between summer and winter ($p > 0.05$). In contrast, at the CIE site, the PM concentrations at the three size ranges were statistically higher in summer than in winter ($p < 0.05$). The site differences may be attributed to the existence of seasonal sources and processes contributing in the summer period to the levels of PM at the urban background site and a rather constant incidence of road traffic emissions at the traffic site in both periods.

In contrast with these results, the values found for PM_{10}, $PM_{2.5}$ and PM_1 mass concentrations in other roadside sites in Toulouse (Calvo et al., 2008), Thessaloniki (Terzi et al., 2010) and Barcelona (Viana et al., 2006), and urban background sites in Zurich (Minguillón et al., 2012) and Ghent (Viana et al., 2007) were, with the exception of Prague (Schwarz et al., 2008), higher in winter than in summer.

In this study, unusually intense clean air mass advections were produced during the winter period, hindering high PM concentration levels. Otherwise, atmospheric conditions facilitated photochemical processes leading to gas to particle conversion during the summer period. In central Spain the frequency of sunny days and solar intensity is clearly higher in summer than in winter. Such is evidenced in the daily average levels of irradiance registered in the CIE meteorological tower (Fig. 2c) in the summer (283.3 W m^{-2}) and in the winter periods (98.8 W m^{-2}). Plaza et al. (1997) demonstrated how the high temperatures and the low wind speeds, frequent in the summer months, trigger the formation and transport of photochemically enriched air in the Madrid air basin.

Various African dust outbreaks were also observed in the summer term. In fact the highest PM concentration values registered in this period were recorded during these dust episodes. At EA, 4 exceedances of the PM_{10} daily limit value (DLV) (50 μg m^{-3}) established by the European Directive 2008/50/EC, were recorded under African dust outbreaks, aside from 2 exceedances produced in the winter period during local pollution events (Fig. 2). At the CIE site, no exceedances of the PM_{10} DLV were registered, neither in summer nor winter. Following the procedure described in Salvador et al. (2013) and references therein, it was concluded that 2 out of the 4 registered exceedances of the PM_{10} DLV in the summer period, could be exclusively attributed to the African dust contribution.

3.3. EC, OC and gaseous pollutants

Mean levels of carbonaceous content determined at the different PM size fractions are shown in Table 1. The size-segregated OC and EC mean values at roadside and urban background sites presented a unimodal distribution in which fine particles enclosed the highest values, except for OC in winter (Fig. 4).

On average, at both sites, OC levels were higher than EC levels in all the size fractions except for the $PM_{0.5}$ during the winter period. The highest concentrations of carbonaceous constituents were obtained at both sites in the $PM_{0.5}$ fraction (Table 1), illustrating the predominant submicrometre nature of OC and EC, which mainly arise from combustion processes and from gas to particle conversion.

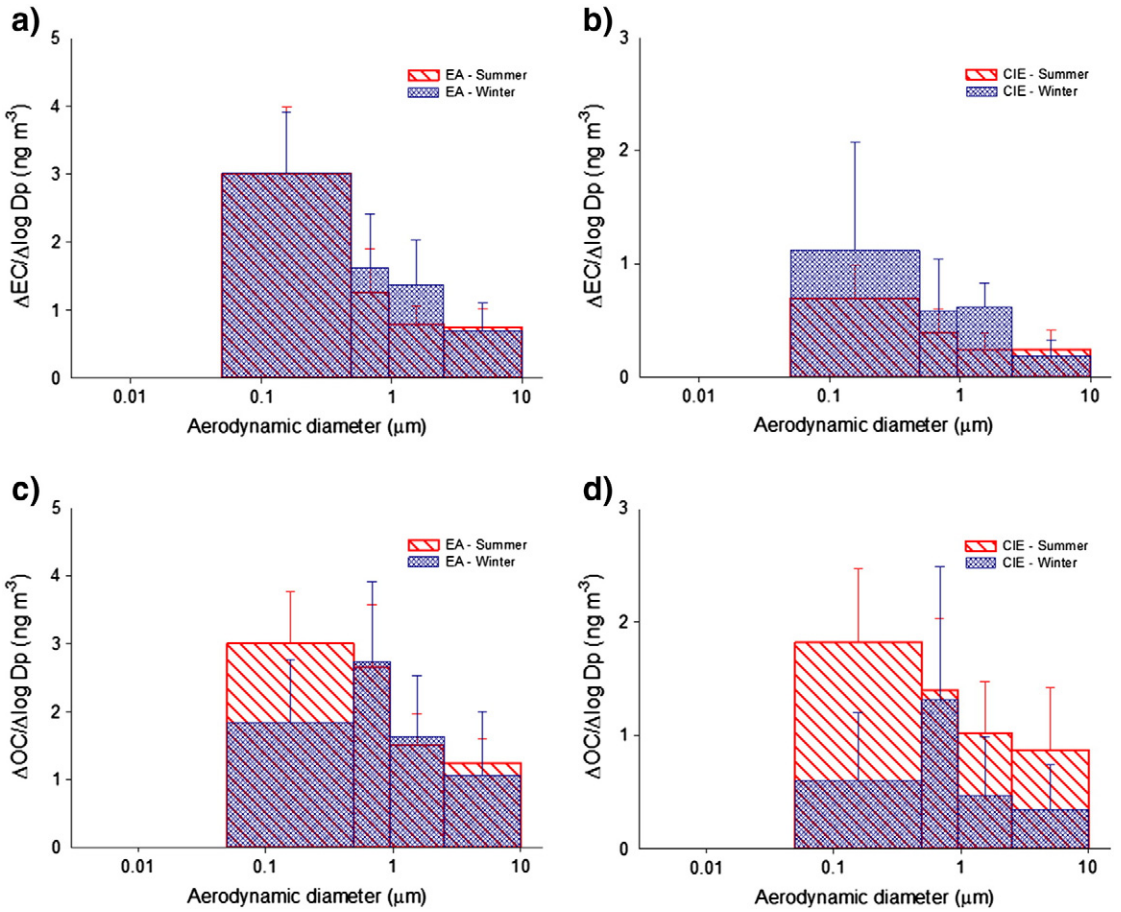

Fig. 4. Average size distributions (plus standard deviations) of EC and OC, in summer and winter (a) at the roadside—EA and (b) at the urban background—CIE.

Cross-correlations between NO_x and EC were high (Fig. 5a), especially during the winter period at both sites ($r^2 = 0.84$-EA; $r^2 = 0.86$-CIE) revealing the primary and traffic-oriented origin of EC, even at the urban background site. Using the sum of the oxidant species $NO_2 + O_3$ as surrogates of secondary gaseous pollutants (Plaza et al. (2006)) a better correlation was obtained at CIE during the summer period, between OC and $NO_2 + O_3$ ($r^2 = 0.60$, Fig. 5b) than between EC and NO_x ($r^2 = 0.50$, not shown). This suggests that, apart from primary combustion emissions, a photochemical secondary origin for a significant fraction of the OC recorded at the urban background site should be considered. In this sense, no consistent seasonal trend was observed for the mean values of EC for the PM_1, $PM_{2.5}$ and PM_{10} size fractions at the EA site. However, the medians of the EC content in these three size fractions at the CIE site were statistically higher in winter than in summer ($p < 0.05$). On the contrary, the OC concentrations were statistically higher in summer than in winter ($p < 0.05$) at both sites.

Statistical tests demonstrated that higher OC and EC values at the different size ranges were observed at the EA site in both seasons. Cross-correlation plots (Fig. 6) between roadside and urban background values show that, in most cases, OC and EC inter-site concentration ratios remain below the 1:1 line. This may indicate that the mean OC and EC levels registered at the CIE site represent the regional contributions in the Madrid region. The addition of the local contributions, from traffic and residential heating, to the regional background, contributes to higher OC and EC levels at EA. The CIE/EA concentration ratios are lower for EC than for OC, evidencing the more local origin of EC emitted by road traffic, and a more regional and secondary origin of OC. At least for summer, the latter, seems to rapidly add to fresh primary vehicle emissions when these are transported from kerbsites to the urban background (Plaza et al., 2011). The CIE/EA ratio for the EC concentrations showed a decrease towards the finest size fraction (Fig. 6a–b), suggesting rapid coagulation of ultrafine EC fresh emissions into larger particles. The mean EC levels at the urban background site, which is more influenced by regional transport of polluted air masses from major traffic routes than by fresh emissions, reveal a lower proportion in submicrometre particles.

A number of OC samples from the coarser fractions appear to be over the 1:1 line, especially during the summer period (Fig. 6c). A possible explanation could be related to the fact that, in summer, OC contributions from biogenic sources increase (Gelencsér et al., 2007). Thus, higher biogenic contributions should be expected at CIE, surrounded by the "Dehesa de la Villa"

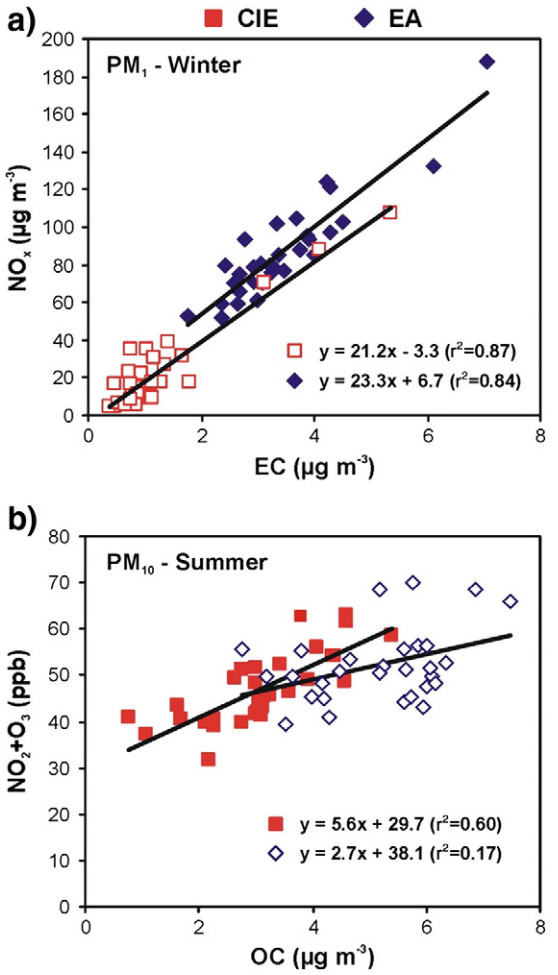

Fig. 5. Cross-correlation between EC and NO_x mean levels (a) and OC and $NO_2 + O_3$ (b) daily mean values recorded at EA and CIE corresponding to the winter (a) and summer (b) periods.

park, than at EA. A complementary explanation is the higher resuspension of road and car break dust containing organic matter, during dry summer periods (Pio et al., 2013).

3.4. Secondary organic aerosol evolution

Whilst EC has only a primary origin from burning of carbonaceous matter, OC may be emitted directly in the particulate phase (POC) or formed from gas to particle conversion processes in the atmosphere (SOC). SOC content still cannot be quantified accurately because of the limited knowledge of its molecular composition, atmospheric processes involved and characteristic emission profiles and its dynamic nature (Pio et al., 2011; Subramanian et al., 2007).

The most commonly accepted method to estimate atmospheric OC, both primary and secondary, relies on the use of EC as a tracer for primary OC concentrations (Castro et al., 1999; Turpin and Huntzicker, 1995). Then, the minimum OC/EC ratio observed may provide estimations of POC, when PM samples containing mostly primary carbonaceous aerosol from fossil fuel combustion are analysed. The OC exceeding that minimum ratio is attributed to secondary sources:

$$SOC = OC - (OC/EC)_{min} EC$$

The existence of a miscellaneous of sources and processes generating different proportions of primary carbon is evidenced in highly variable OC/EC minimum ratios. A low OC-to-EC ratio has been associated with traffic sources (2.2 and 0.8 for light-duty gasoline and heavy-duty diesel vehicles, respectively), whereas residential heating (wood combustion 4.15 and natural gas home appliances 12.7), forest fires (14.5) and dust from paved roads (13.1) have shown remarkably higher ratios (Sillanpaa et al., 2005). Viana et al. (2006) pointed out that variations in time series of the OC/EC ratios can be interpreted as changes in emission sources strengths or source regions. A high variability in the OC/EC ratios by meteorological conditions was also documented by Salma et al. (2005).

In this study, it has been observed that the OC/EC ratio does not show great variations during the winter period. In contrast, during the summer, different synoptic meteorological situations, contributed to sudden changes in the ratio (Table 2). In order to check the significance of inter-synoptic meteorological situation variations in the OC/EC ratio, Kruskal–Wallis non-parametric tests were applied. The test results indicated that statistically significant differences in the OC/EC ratio in winter were not observed for the different synoptic situations at the 99% confidence level at both sites (Fig. 7). Besides, no statistically significant correlation ($p > 0.1$) between the daily OC/EC ratios and the daily mean levels of NO, CO and O_3 in PM_{10}, $PM_{2.5}$ and PM_1 was found during this term. This means that, from the meteorological point of view, unlike the levels of these gaseous pollutants, the ratio remained fairly unchanged across the different periods identified. Thus, a predominant primary carbon source influencing the area, as well as lower levels of SOA formation, contributes to less variable OC/EC ratios in wintertime. Taking into account the traffic emission results of Pio et al. (2013) and the discussion in Pio et al. (2011), any OC with an origin in gas to particle conversion would result predominantly from rapid condensation of semi-volatile organic compounds at the lower temperatures prevalent in the cold season.

Then, the use of the (OC/EC) minimum ratio to obtain estimates of POC can be considered reasonable in this particular case. The procedure described in Pio et al. (2011) was used.

$(OC/EC)_{min}$ ratios obtained for PM_{10} (0.55 and 0.35 at EA and CIE, respectively) and $PM_{2.5}$ (0.30 and 0.33 at EA and CIE, respectively) were lower than the typical $(OC/EC)_{min}$ ratios attributed to fossil fuel (1.0 and 0.7) at many urban background sites in Europe and, excluding the PM_{10}–EA ratio, within the ranges obtained in a roadway tunnel in Lisbon (0.33–0.42 for PM_{10} and 0.29–0.37 for $PM_{2.5}$) (Pio et al., 2011). This evidences that the minimum ratios obtained are good estimations of the pure OC/EC from fossil fuel combustion in Madrid. In the case of the lowest fractions, the estimated $(OC/EC)_{min}$ ratio was 0.29 at both sites for PM_1 and 0.24 at EA and 0.20 at CIE for $PM_{0.5}$. The results for seasonal and total data, obtained with basis on the $(OC/EC)_{min}$ ratios at each particle size range, are exhibited in Table 2. These results falls in the ranges of SOC content of OC in $PM_{2.5}$ estimated with a different methodology at CIE, by Plaza et al. (2011) for different months of the 2006–2008 period.

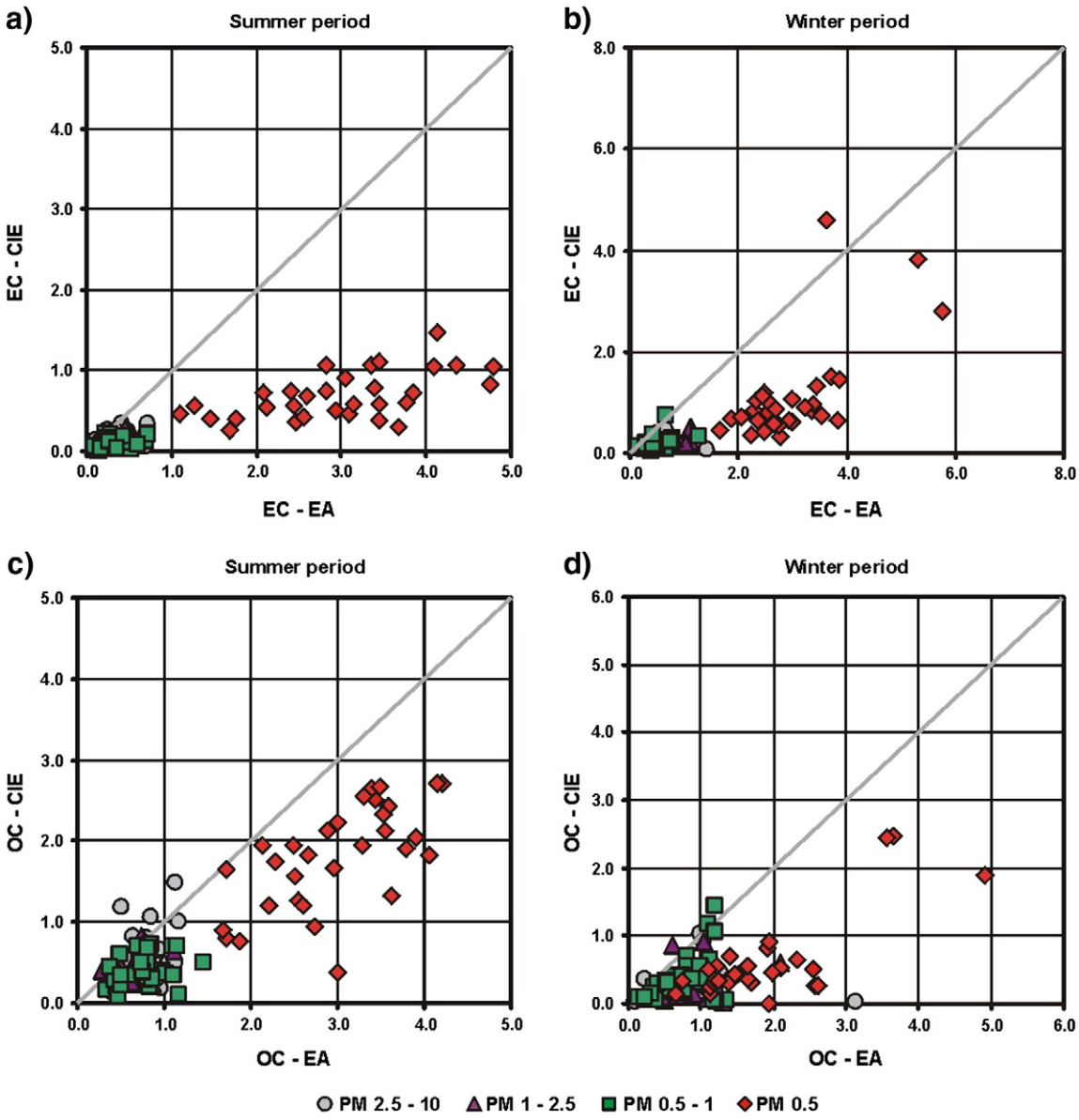

Fig. 6. Cross-correlations between daily EC (a–b) and OC (c–d) levels (μg m^{-3}) recorded at the EA and CIE sites in the summer and winter periods.

SOC data show a clear seasonal pattern. Much higher SOC concentration values were obtained in summer than in winter at both sites (>50% at CIE). In relative terms, the SOC content of particulate OC was higher at the urban background than at the urban traffic site and at the lower particle size ranges (Table 2). This tendency reflects the lower incidence of primary OC emissions from fossil fuel combustion and road dust in the CIE urban background site as well as the transport by regional circulations (Plaza et al., 1997) of secondary OC from the more polluted areas of the centre of Madrid and its surrounding traffic lanes. Lower concentrations of SOC during summer periods were obtained in PM_1, $PM_{2.5}$ and PM_{10} at a roadside and an urban background sites in the UK (Harrison and Yin, 2008) and in $PM_{2.5}$ at an urban traffic-influenced site in Helsinki, Finland (Viidanoja et al., 2002). These results are suggestive of the prevailing photochemical origin for the SOC recorded in the Madrid air basin, under typical favourable atmospheric conditions in the summer period. As a consequence, most of the OC in the finest fraction, $PM_{0.5}$, was SOC during this term (Table 2).

3.5. Ion balance: formation of coarse and fine secondary inorganic compounds

In general, the levels of most ions were higher at EA than at CIE (Table 1). At both sampling sites and seasons, the secondary NO_3^- and SO_4^{2-} ions dominated in every size fraction, followed by the primary Ca^{2+} and Na^+.

Some differences in the ion concentrations between summer and winter were observed. Results of the Mann–Whitney tests showed that crustal ions Ca^{2+} and Mg^{2+}, as well as SO_4^{2-}, presented statistically significant higher values ($p < 0.01$) in

Table 2
Mean OC/EC ratios found in the ambient air of Madrid and average concentrations (μgC m^{-3}) for secondary OC (SOC) and primary OC (POC), estimated from OC/EC minimum ratios, distributed in four size classes.

		EA			CIE	
	Whole	Summer	Winter	Whole	Summer	Winter
PM_{10}						
OC/EC[a]	1.1 ± 0.4	1.3 ± 0.4	0.9 ± 0.2	2.0 ± 1.4	3.2 ± 1.0	0.8 ± 0.3
SOC[b]	2.6 (57%)	3.2 (64%)	1.9 (49%)	1.8 (79%)	2.8 (88%)	0.8 (58%)
POC	1.9	1.8	2.0	0.5	0.4	0.6
$PM_{2.5}$						
OC/EC	1.0 ± 0.4	1.3 ± 0.4	0.8 ± 0.3	1.9 ± 1.4	3.1 ± 0.9	0.7 ± 0.3
SOC	2.5 (65%)	3.1 (71%)	1.8 (57%)	1.5 (79%)	2.3 (89%)	0.7 (57%)
POC	1.3	1.3	1.4	0.4	0.3	0.5
PM_{1}						
OC/EC	1.0 ± 0.4	1.2 ± 0.4	0.8 ± 0.3	1.8 ± 1.3	2.9 ± 0.8	0.8 ± 0.3
SOC	2.2 (69%)	2.8 (74%)	1.6 (62%)	1.3 (82%)	2.0 (90%)	0.6 (65%)
POC	1.0	1.0	1.0	0.3	0.2	0.3
$PM_{0.5}$						
OC/EC	0.8 ± 0.4	1.1 ± 0.4	0.6 ± 0.2	1.7 ± 1.3	2.7 ± 0.8	0.5 ± 0.2
SOC	1.8 (75%)	2.4 (80%)	1.2 (67%)	1.0 (86%)	1.7 (92%)	0.4 (65%)
POC	0.6	0.6	0.6	0.2	0.1	0.2

[a] Mean ± standard deviation.
[b] Percentage of secondary OC in brackets.

summer than winter, at both sites, in PM_{10}, $PM_{2.5}$ and PM_1. Within the Iberian Peninsula, crustal material concentrations are usually higher in summer, not only due to local–regional dust resuspension from road traffic and wind blowing, but also by the more frequent occurrence of African dust outbreaks (Salvador et al., 2013). Complementarily, SO_4^{2-} levels are at their maximum in summer because of the stronger insulation and the ensuing higher oxidation of SO_2 to SO_4^{2-} (Querol et al., 2008). On the contrary, higher values ($p < 0.01$) in winter than summer were obtained for the secondary species NO_3^- and NH_4^+, in the finest size fractions, and for Cl^- and Na^+ in PM_{10} and $PM_{2.5}$ at the EA site. The more efficient transport from the Atlantic, and the spreading of salt on the road lanes to melt the ice and snow during the winter period, explain the seasonal behaviour of Na^+ and Cl^- in coarse particles. The seasonality of ammonium and nitrate may be explained by the thermal stability of ammonium nitrate: given a neutralisation of NO_3^- by the available NH_4^+ after most of SO_4^{2-} has been neutralised, nitrate aerosol has the form of NH_4NO_3, whose formation is reversible, being subject to vaporation, thus leading to lower summer concentrations. The K^+ ion does not show any seasonality at both sites, suggesting a regional origin.

The ion balance expressed by the sum of the equivalent concentration (μeq m^{-3}) ratio of cations to anions may be used as an indicator to verify the reliability and accuracy of the measured concentrations (Wang et al., 2005). The ratios in all fractions, except in the 2.5–10, are close to unity, indicating that the major ions were quantified and that the data may be considered as accurate. An excess in the amount of cations with respect to anions was observed at both sites in summer in the coarse fraction, which might be explained by an excess of carbonates in this period. The inclusion in the balance of carbonate concentrations measured in coarser size fractions demonstrates that this is the reason for the cation excess.

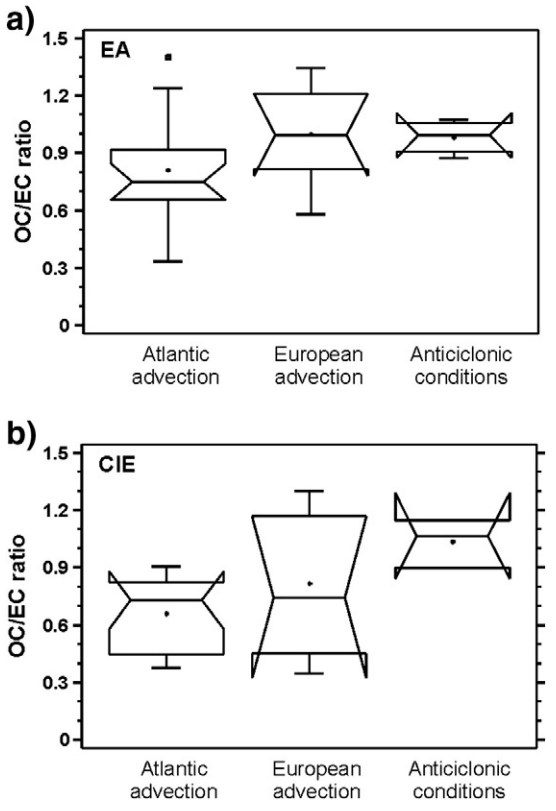

Fig. 7. Boxplots of the PM_{10} OC/EC ratio values in EA (a) and CIE (b). The data are divided into four quartiles. Median is drawn as a horizontal line inside the box. Boxplot notches describe the expected range of variability of the median. If the notches of two boxes do not overlap, this offers evidence of a statistically significant difference between the medians.

A compound balance for each size stage was computed from the measured water soluble ion concentrations, inspired in the work presented by Alastuey et al. (2005) and based in commonly accepted atmospheric reaction processes. The following rules were applied:

(1) Na^+ was considered to originate only from sea salt (with a marine origin or from road deicing) and was firstly balanced with sulphate to form sodium and magnesium sea salt sulphates, with ratios dependent from sea salt composition;
(2) excess (free) sodium and magnesium are associated with chloride in proportions equivalent to sea water, until any of the ions (generally chloride) is totally spent;
(3) NH_4^+ is preferentially associated with free (non sea salt) SO_4^{2-}, as $(NH_4)_2SO_4$ (Seinfeld and Pandis, 1998); in the case of an excess of NH_4^+ with respect to SO_4^{2-}, the free NH_4^+ is balanced firstly with NO_3^- and secondly with Cl^-, to form ammonium nitrate and chloride;
(4) any free NO_3^-, after balancing with NH_4^+, is associated sequentially with sea salt cations (free Na^+ and Mg^{2+}, after step (2)), in proportions equivalent to sea water, and with soil cations (Ca^{2+}, K^+, and Mg^{2+});
(5) any free SO_4^{2-} is also sequentially associated with free sea salt and soil cations (Na^+, Mg^{2+}, Ca^{2+}, and K^+); if any SO_4^{2-} remains free after this step it is considered as non-reacted sulphuric acid;
(6) any free Cl^-, after steps (2) and (3), is sequentially associated with Ca^{2+} and K^+, being supposed to result from soil or from reaction of gaseous HCl with soil particles;
(7) after previous balances any free Ca^{2+}, Mg^{2+} and K^+ are considered as non-reacted soil particles; two methodologies are followed for these free ions: if carbonate was measured, the cations are sequentially associated with CO_3^{2-} until any of the ions is completely spent; if carbonate was not measured all these free cations are considered as carbonated salts.

Sea salt levels were similar at EA and CIE in summer. In the cold season, sea salt particles were present at higher concentrations at the roadside than at urban background, likely due to resuspension of road dust containing deicing salt. One important part of chlorine seems to have been evaporated from sea salt particles at both sites, principally for sizes <2.5 μm in summer, probably as a result of the attack by less volatile nitric and sulphuric acids (Pio and Lopes, 1998). Results are shown in Table 3.

Albeit detected in all fractions, $(NH_4)_2SO_4$, presented higher concentrations in the smaller grain sizes (Harrison and Pio, 1983). At both sites more than 90% and 75% of $(NH_4)_2SO_4$, were present in the PM_1 fraction in the summer and the winter periods, respectively. NH_4NO_3 was almost exclusively detected in winter. During this season, 89% and 82% of the NH_4NO_3 determined in EA and CIE, respectively, were present in the submicrometre (<1 μm) fraction. It was also observed that, during winter, principally in EA, the formation of small amounts of NH_4Cl in submicrometre particles may occur.

Due to the high volatility of ammonium nitrates at high temperatures and low humidity (Harrison and Kitto, 1990), no NH_4NO_3 was obtained in summer for any grain size. It was found that, in summertime, particulate nitrate existed in association with sea salt and soil cations, in general distributed homogeneously between fine and coarse fractions. This is probably resultant from reactions involving photochemically originated nitric acid and both sea salt and soil particles. In winter, the reaction of nitric acid with sea salt and soil dust also took place at both sites, but less intensively. The reaction of HNO_3 with sea salt NaCl, or with soil carbonates, has been reported in the literature (Brimblecombe and Clegg, 1988; Harrison and Pio, 1983; Mamane and Gottlieb, 1992; Pakkanen, 1996; Wall et al., 1988).

Important quantities of sulphates were also associated with soil cations such as calcium, especially in summer. Calcium sulphate was uniformly distributed across the four size ranges and seems therefore to be originated from both the attack of SO_2 and sulphuric acid on soil compounds and from the existence of sulphate in the soil. Principally in the smaller size range and during summer, an excess amount of sulphate that could not be compensated by any of the cations measured was verified, indicating the presence of unreacted sulphuric acid or non-totally neutralised ammonium bi-sulphates. The levels of acidic sulphates were higher at the urban background site where there was less dust from road resuspension to neutralise the regionally formed acids.

In the winter period most of the $CaSO_4$ was estimated to be present in the coarser fraction (2.5–10 μm), whereas in the summer term, it was also detected in the smaller size fractions. In fact, 56% and 42% of the $CaSO_4$ determined in EA and CIE, respectively, were concentrated in the submicrometre fractions. In summer, a similar pattern was observed for $Ca(NO_3)_2$, for which 53% and 70% of the mass were concentrated in submicrometre particles, respectively at EA and CIE. This is likely associated with the unusual presence in the atmosphere of Madrid of a significant content of Ca^{2+} and, in a lesser amount, of Mg^{2+}, K^+ and Na^+, in the submicrometric fraction during the summer period. Pio et al. (2013) found predominant amounts of calcium and sodium in submicrometre particles resulting from traffic emissions, in an urban road tunnel in Lisbon. Moreno et al. (2013) demonstrated that the concentration of inhalable mineral dust in Madrid is strongly influenced by traffic suspension or resuspension. They showed a high correlation between daily profiles of hourly concentrations of Al and Ca (obtained by a Streaker sampler in the 0.1–2.5 and 2.5–10 μm size ranges), PM_{10}, NO_2 and Cu, Zn and Cr in the EA traffic hot-spot monitoring site. These authors also found a calcium rich group of particles in the fine range, associated with construction and roadwork activities and subsequent traffic road dust resuspension in the Escuelas Aguirre site. The presence of $CaCO_3$ and Na_2CO_3 in the fine modes may also be a consequence of their use as antacids in lubricating oils (Cahill et al., 2007).

It should be taken into account that the summer period was affected by frequent African dust outbreaks. These events, especially those produced in the 2–3 June and 12–19 June periods, clearly influenced the levels of Ca^{2+}. Mean values of Ca^{2+} were considerably higher during dusty days than during non-dusty days (Fig. 8) and did not coincide with the highest concentrations of carbonates. Differences ranged from 56% higher values in dusty days in the <0.5 fraction to 214% higher values in the 1–2.5 fraction, at the CIE site. At the EA traffic site, differences were less extreme (from 20% higher in dusty days

Table 3
Concentrations and estimated composition of WSIM, by size, in summer and winter at the roadside and urban background.

	$PM_{0.5}$		$PM_{0.5-1}$		$PM_{1-2.5}$		$PM_{2.5-10}$	
	Sum.	Win.	Sum.	Win.	Sum.	Win.	Sum.	Win.
Roadside								
Cations (neq m^{-3})	23.4	29.7	9.7	12.5	9.0	17.2	10.8	25.5
Anions (neq m^{-3})	24.0	23.0	8.0	10.9	12.2	15.5	20.2	24.2
Estimation (μg m^{-3})								
$(Na_2)_{ss}SO_4$	0.021	0.025	0.012	0.014	0.020	0.039	0.028	0.11
$(Mg)_{ss}SO_4$	0.0040	0.0048	0.0046	0.0040	0.050	0.017	0.010	0.036
$(Na)_{ss}Cl$	0.062	0.12	0.024	0.072	0.038	0.23	0.11	0.68
$(Mg)_{ss}Cl$	0.010	0.011	0.0040	0.0062	0.0071	0.021	0.020	0.038
$(NH_4)_2SO_4$	0.64	0.54	0.21	0.24	0.049	0.17	0.012	0.0094
NH_4NO_3		0.87		0.34		0.15		0.00036
NH_4Cl		0.018		0.0017				
$NaNO_3$	0.13	0.035	0.093	0.041	0.18	0.099	0.16	0.16
$Mg(NO_3)_2$	0.035	0.0030	0.019	0.0022	0.047	0.0049	0.043	0.00034
$Ca(NO_3)_2$	0.31	0.021	0.019	0.056	0.065	0.19	0.22	0.063
KNO_3	0.0071			0.0031		0.015	0.0046	
$CaSO_4$	0.24		0.16	0.0020	0.18	0.022	0.13	0.080
K_2SO_4	0.023		0.0064		0.033	0.00062	0.014	
Na_2SO_4								
$MgSO_4$			0.0013		0.00067		0.00081	
H_2SO_4	0.056		0.0057		0.011		0.023	
$CaCl_2$	0.019	0.0050	0.0016	0.0076	0.00068	0.022	0.00025	0.10
KCl	0.0082			0.0025		0.0019	0.00019	0.0010
$CaCO_3$	0.062	0.20	0.058	0.047	0.027	0.072	0.020	0.075
$MgCO_3$	0.00089	0.0041	0.010	0.0012			0.00040	
K_2CO_3	0.026	0.060	0.021	0.025	0.018	0.026	0.020	0.0074
Urban background								
Cations (neq m^{-3})	19.7	17.4	8.1	9.4	8.3	10.9	9.7	12.5
Anions (neq m^{-3})	24.5	15.2	6.1	9.3	9.1	10.1	15.4	16.9
Estimation (μg m^{-3})								
$(Na_2)_{ss}SO_4$	0.032	0.010	0.0072	0.0094	0.026	0.026	0.025	0.055
$(Mg)_{ss}SO_4$	0.062	0.0019	0.0014	0.0034	0.010	0.010	0.0089	0.017
$(Na)_{ss}Cl$	0.13	0.031	0.014	0.033	0.030	0.13	0.037	0.36
$(Mg)_{ss}Cl$	0.012	0.0015	0.0026	0.0050	0.0056	0.020	0.0068	0.036
$(NH_4)_2SO_4$	0.54	0.36	0.21	0.22	0.045	0.14	0.010	0.0081
NH_4NO_3	0.011	0.60	0.0016	0.17	0.0029	0.16		0.0013
NH_4Cl		0.0031		0.00024				
$NaNO_3$	0.15	0.035	0.053	0.032	0.20	0.11	0.21	0.093
$Mg(NO_3)_2$	0.015	0.0022	0.017	0.0033	0.042	0.0077	0.044	0.00012
$Ca(NO_3)_2$	0.32	0.052	0.032	0.063	0.061	0.089	0.094	0.064
KNO_3	0.018	0.0044		0.034		0.0089	0.0018	
$CaSO_4$	0.066	0.0068	0.071	0.0039	0.11	0.0066	0.080	0.022
K_2SO_4	0.049	0.0059	0.0055		0.0088	0.00033	0.0025	
Na_2SO_4	0.018	0.0027	0.00042					
$MgSO_4$	0.0013		0.0015		0.00020			
H_2SO_4	0.17	0.0061	0.0035		0.0031		0.0045	
$CaCl_2$	0.0089	0.00090	0.00032	0.00038		0.0028		0.031
KCl	0.00068	0.0040				0.0011		0.0020
$CaCO_3$	0.0086	0.042	0.076	0.022	0.033	0.027	0.046	0.046
$MgCO_3$	0.0011	0.0011	0.0068	0.0010	0.0038	0.0058	0.011	
K_2CO_3	0.0043	0.034	0.017	0.016	0.010	0.012	0.013	0.012

ss—sea salt.

than non-dusty days at the <0.5 fraction to 94% higher at the 2.5–10 fraction) pointing out a significant influence of the dust resuspension processes mentioned earlier. Deposition of highly disaggregated $CaCO_3$ mineral particles during these events could be the main reason why the average concentration of Ca^{2+} in summer, at both sampling sites, was higher in the smaller size fractions. Besides, small particles constituted by Ca sulphates (dust particles coated with sulphate) have been previously detected, coming from African dust plumes (Alastuey et al., 2005; Kandler et al., 2007). Đorđević et al. (2012) also obtained a bimodal size distribution for Ca^{2+}, with one mode at $Dp \leq 0.49$ μm and the other one at $3.0 \leq Dp \leq 7.2$ μm in the city centre of Belgrade, in the Balkan region.

4. Conclusions

This work reports the carbonaceous content and the ionic composition of size-segregated fractions of the urban aerosol in Madrid. Concentrations of carbon forms (EC and OC) and the major water soluble ions (Cl^-, NO_3^-, SO_4^{2-}, Na^+, NH_4^+, K^+, Mg^{2+} and Ca^{2+}) were measured for a total of 30 samples in

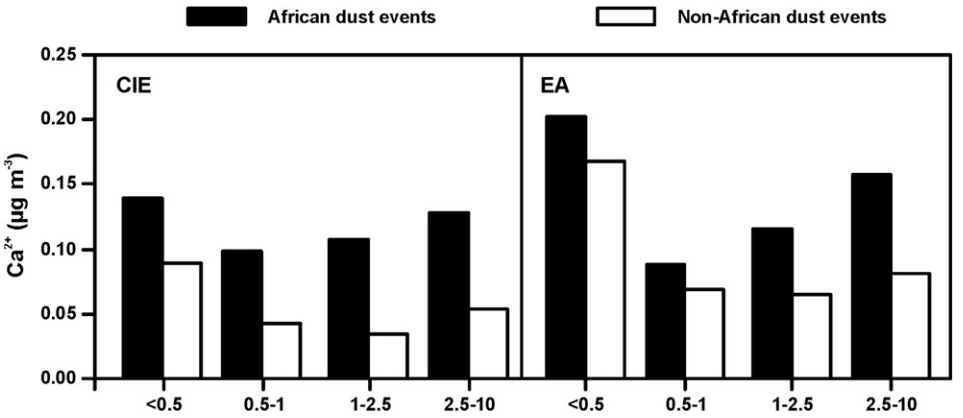

Fig. 8. Average concentration of Ca^{2+} in the various fractions at the roadside (EA) and urban background (CIE) during African dust episodic days and the other days in the summer period.

each sampling site (urban background and roadside) and season (summer and winter) comprising four size fractions.

The PM_{10} mass was found predominantly in the ultrafine (<0.5) and, to a lesser extent, the coarse (2.5–10) fractions at both sites. The highest concentrations of EC and OC were obtained at both sites in the $PM_{0.5}$, illustrating the predominantly submicrometre nature of these carbonaceous constituents, which arise predominantly from combustion processes and from gas to particle conversion.

In this study, many different synoptic meteorological situations were registered, spanning from unusually intense clean air mass advections and cold waves produced during the winter period to stagnant anticyclone conditions and frequent African dust outbreaks in the summer period. The strong and rather constant incidence of road traffic emissions at the urban traffic site is reflected in the fact that there was not a statistically significant difference between the PM and the EC concentrations at the different grain sizes in summer and winter. In contrast, at the urban background site, PM and OC concentrations at three size ranges were higher in summer than in winter, unlike the EC concentrations, which were higher in winter than summer. The inter-site differences may be attributed to the existence of new sources and processes contributing in the summer period to the levels of PM at the urban background site apart from road traffic emissions, such as secondary organic aerosol production from photo-oxidation of both biogenic and anthropogenic volatile organic compounds. Estimation of secondary and primary OC concentrations using the EC tracer method revealed much higher average concentrations of secondary OC in summer than winter at both sites, as well as higher relative contributions at the urban background than at the road traffic site.

In relation to the characterisation of the ionic composition of the particulate matter in Madrid, the secondary ions NO_3^- and SO_4^{2-} dominated in all size fractions in both sampling sites and seasons. $(NH_4)_2SO_4$ levels were at their maximum at both sites in summer in the submicrometre fraction as a consequence of the favourable atmospheric conditions for the generation of photochemical reactions in the Madrid air basin. On the contrary, higher values were obtained in winter than summer, for ultrafine NH_4NO_3 and coarse NaCl, the former due to the spreading of salt on the road lanes to melt the ice and snow during the cold period.

As a result of the unusual presence in the atmosphere of Madrid of a substantial content of Ca^{2+} in the submicrometric fraction during the summer period, an elevated percentage of $CaSO_4$ was determined in EA and CIE, in the smaller size fractions. It was mainly attributed to a calcium rich group of highly disaggregated particles in the fine range, associated with construction and roadwork activities and subsequent traffic road dust resuspension in the urban traffic site and to African dust contributions. These events, especially those produced in the 2–3 June and 12–19 June periods, clearly influenced the levels of Ca^{2+} registered at both sites.

Acknowledgements

F. Mirante thanks the Portuguese Science Foundation for the financial support of the training period at CIEMAT, as well for the PhD grant SFRH/BD/45473/2008. This work has also been partially carried out under the framework of the Acción Integrada PT2009-0151, CGL2011-27020 project funded by the Spanish Ministry of Science and Innovation and Action nº E-130/10 funded by CRUP. The authors also thank everybody who helped during the sampling campaigns. The authors would also like to thank the NOAA/OAR/ESRL PSD, Boulder, Colorado, USA for providing the meteorological dataset files (www.cdc.noaa.gov/) used for the composition of the synoptic situations.

References

Alastuey, A., Querol, X., Castillo, S., Escudero, M., Avila, A., Cuevas, E., Torres, C., Romero, P.-M., Exposito, F., García, O., Pedro Diaz, J., Dingenen, R.V., Putaud, J.P., 2005. Characterisation of TSP and $PM_{2.5}$ at Izaña and Sta. Cruz de Tenerife (Canary Islands, Spain) during a Saharan Dust Episode (July 2002). Atmos. Environ. 39, 4715–4728.

Aldabe, J., Elustondo, D., Santamaría, C., Lasheras, E., Pandolfi, M., Alastuey, A., Querol, X., Santamaría, J.M., 2011. Chemical characterisation and source apportionment of $PM_{2.5}$ and PM_{10} at rural, urban and traffic sites in Navarra (North of Spain). Atmos. Res. 102, 191–205.

Almeida, E., 2009. Aerosol carbonoso: contribuiçao para a sua caraterização. (Master Thesis) Aveiro University.

Alves, C.A., Gonçalves, C., Pio, C.A., Mirante, F., Caseiro, A., Tarelho, L., Freitas, M.C., Viegas, D.X., 2010. Smoke emissions from biomass burning in a Mediterranean shrubland. Atmos. Environ. 44, 3024–3033.

Artıñano, B., Salvador, P., Alonso, D.G., Querol, X., Alastuey, A., 2003. Anthropogenic and natural influence on the PM_{10} and $PM_{2.5}$ aerosol in Madrid (Spain). Analysis of high concentration episodes. Environ. Pollut. 125, 453–465.

Ayuntamiento, M., 2010. Inventario de emisiones de contaminantes a la atmósfera en el municipio de Madrid. 1990–2008.
Brimblecombe, P., Clegg, S.L., 1988. The solubility and behaviour of acid gases in the marine aerosol. J. Atmos. Chem. 7, 1–18.
Cahill, T., Cahill, T., Spada, N., Barnes, D., Cliff, S., Perry, K., Fujii, E., 2007. Mass, elemental, and organic aerosols by size, time, and composition for the Roseville Railyard Aerosol Monitoring Project (RRAMP). Final report.
Calvo, A.I., Pont, V., Liousse, C., Dupré, B., Mariscal, A., Zouiten, C., Gardrat, E., Castera, P., Lacaux, C.G., Castro, A., Fraile, R., 2008. Chemical composition of urban aerosols in Toulouse, France during CAPITOUL experiment. Meteorol. Atmos. Phys. 102, 307–323.
Calvo, A.I., Alves, C., Castro, A., Pont, V., Vicente, A.M., Fraile, R., 2013. Research on aerosol sources and chemical composition: past, current and emerging issues. Atmos. Res. 120–121, 1–28.
Cancio, J., Castellano, A., Martín, S., Rodríguez, J., 2004. Size distributions of PAHs in ambient air particles of two areas of Las Palmas de Gran Canaria. Water Air Soil Pollut. 154, 127–138.
Castro, L.M., Pio, C.A., Harrison, R.M., Smith, D.J.T., 1999. Carbonaceous aerosol in urban and rural European atmospheres: estimation of secondary organic carbon concentrations. Atmos. Environ. 33, 2771–2781.
Chow, J.C., Watson, J.G., Chen, L.W.A., Chang, M.C.O., Paredes-Miranda, G., 2005. Comparison of the DRI/OGC and Model 2001 Thermal/Optical Carbon Analyzers. Final Report for the IMPROVE Steering Committee. Desert Research Institute, Reno, NV, USA.
Costa, E.A., Campos, V.P., Da Silva Filho, L.C., Greven, H.A., 2009. Evaluation of the aggressive potential of marine chloride and sulfate salts on mortars applied as renders in the Metropolitan Region of Salvador—Bahia, Brazil. J. Environ. Manag. 90, 1060–1068.
Das, S.K., Jayaraman, A., 2012. Long-range transportation of anthropogenic aerosols over eastern coastal region of India: investigation of sources and impact on regional climate change. Atmos. Res. 118, 68–83.
Donahue, N.M., Robinson, A.L., Pandis, S.N., 2009. Atmospheric organic particulate matter: from smoke to secondary organic aerosol. Atmos. Environ. 43, 94–106.
Đorđević, D., Mihajlidi-Zelić, A., Relić, D., Ignjatović, L., Huremović, J., Stortini, A.M., Gambaro, A., 2012. Size-segregated mass concentration and water soluble inorganic ions in an urban aerosol of the Central Balkans (Belgrade). Atmos. Environ. 46, 309–317.
Draxler, R.R., Rolph, G.D., 2003. *HYSPLIT (HYbrid Single-Particle Lagrangian Integrated Trajectory)* [Online]. MD. Model access via NOAA ARL READY Website. (http://www.arl.noaa.gov/ready/hysplit4.html).
Duan, J., Bi, X., Tan, J., Sheng, G., Fu, J., 2005. The differences of the size distribution of polycyclic aromatic hydrocarbons (PAHs) between urban and rural sites of Guangzhou, China. Atmos. Res. 78, 190–203.
E.E.A. (European Environment Agency), 1999. Environment in the European Union at the turn of the century. Environmental assessment report No 2.
Gelencsér, A., May, B., Simpson, D., Sánchez-Ochoa, A., Kasper-Giebl, A., Puxbaum, H., Caseiro, A., Pio, C., Legrand, M., 2007. Source apportionment of $PM_{2.5}$ organic aerosol over Europe: primary/secondary, natural/anthropogenic, and fossil/biogenic origin. J. Geophys. Res. 112, 1–12.
Gillies, J.A., Gertler, A.W., 2000. Comparison and evaluation of chemically speciated mobile source $PM_{2.5}$ particulate matter profiles. J. Air Waste Manag. Assoc. 50, 1459–1480.
Gómez-Moreno, F.J., Núñez, L., Plaza, J., Alonso, D., Pujadas, M., Artíñano, B., 2007. Annual evolution and generation mechanisms of particulate nitrate in Madrid. Atmos. Environ. 41, 394–406.
Harrison, R.M., Kitto, A.-M.N., 1990. Surface-exchange of atmospheric nitrogen species including nitrous acid. Presented at the 7th International Symposium of the Commission on Atmospheric Chemistry and Global Pollution. Chamrousse, France.
Harrison, R.M., Pio, C.A., 1983. Size-differentiated composition of inorganic atmospheric aerosols of both marine and polluted continental origin. Atmos. Environ. 17, 1733–1738.
Harrison, R.M., Yin, J., 2008. Sources and processes affecting carbonaceous aerosol in central England. Atmos. Environ. 42, 1413–1423.
Ito, K., Mathes, R., Ross, Z., Nádas, A., Thurston, G., Matte, T., 2011. Fine particulate matter constituents associated with cardiovascular hospitalizations and mortality in New York City. Environ. Health Perspect. 119, 467–473.
Kalnay, E., Kanamitsu, M., Kistler, R., Collins, W., Deaven, D., Gandin, L., Iredell, M., Saha, S., White, G., Woollen, J., Zhu, Y., Leetmaa, A., Reynolds, R., Chelliah, M., Ebisuzaki, W., Higgins, W., Janowiak, J., Mo, K.C., Ropelewski, C., Wang, J., Jenne, R., Joseph, D., 1996. The NCEP/NCAR 40-year reanalysis project. Bull. Am. Meteorol. Soc. 77, 437–471.
Kandler, K., Benker, N., Bundke, U., Cuevas, E., Ebert, M., Knippertz, P., Rodríguez, S., Schütz, L., Weinbruch, S., 2007. Chemical composition and complex refractive index of Saharan Mineral Dust at Izaña, Tenerife (Spain) derived by electron microscopy. Atmos. Environ. 41, 8058–8074.
Katul, G.G., Grönholm, T., Launiainen, S., Vesala, T., 2011. The effects of the canopy medium on dry deposition velocities of aerosol particles in the canopy sublayer above forested ecosystems. Atmos. Environ. 45, 1203–1212.
Lighty, J.S., Veranth, J.M., Sarofim, A.F., 2000. Combustion aerosols: factors governing their size and composition and implications to human health. J. Air Waste Manag. Assoc. 50, 1565–1619.
Mamane, Y., Gottlieb, J., 1992. Nitrate formation on sea-salt and mineral particles—a single particle approach. Atmos. Environ. Part A 26, 1763–1769.
Minguillón, M.C., Querol, X., Baltensperger, U., Prévôt, A.S.H., 2012. Fine and coarse PM composition and sources in rural and urban sites in Switzerland: local or regional pollution? Sci. Total Environ. 427–428, 191–202.
Moreno, T., Karanasiou, A., Amato, F., Lucarelli, F., Nava, S., Calzolai, G., Chiari, M., Coz, E., Artíñano, B., Lumbreras, J., Borge, R., Boldo, E., Linares, C., Alastuey, A., Querol, X., Gibbons, W., 2013. Daily and hourly sourcing of metallic and mineral dust in urban air contaminated by traffic and coal-burning emissions. Atmos. Environ. 68, 33–44.
Oliveira, C., Pio, C., Caseiro, A., Santos, P., Nunes, T., Mao, H., Luahana, L., Sokhi, R., 2010. Road traffic impact on urban atmospheric aerosol loading at Oporto, Portugal. Atmos. Environ. 44, 3147–3158.
Pakkanen, T.A., 1996. Study of formation of coarse particle nitrate aerosol. Atmos. Environ. 30, 2475–2482.
Pio, C.A., Lopes, D.A., 1998. Chlorine loss from marine aerosol in a coastal atmosphere. J. Geophys. Res. Atmos. 103, 25263–25272.
Pio, C., Cerqueira, M., Harrison, R.M., Nunes, T., Mirante, F., Alves, C., Oliveira, C., Campa, A.S.D.L., Artíñano, B., Matos, M., 2011. OC/EC ratio observations in Europe: re-thinking the approach for apportionment between primary and secondary organic carbon. Atmos. Environ. 45, 6121–6132.
Pio, C., Mirante, F., Oliveira, C., Matos, M., Caseiro, A., Oliveira, C., Querol, X., Alves, C., Martins, N., Cerqueira, M., Camões, F., Silva, H., Plana, F., 2013. Size-segregated chemical composition of aerosol emissions in an urban road tunnel in Portugal. Atmos. Environ. 71, 15–25.
Plaza, J., Pujadas, M., Artíñano, B., 1997. Formation and transport of the Madrid ozone plume. J. Air Waste Manag. Assoc. 47, 766–774.
Plaza, J., Gómez-Moreno, F.J., Núñez, L., Pujadas, M., Artíñano, B., 2006. Estimation of secondary organic aerosol formation from semi-continuous OC–EC measurements in a Madrid suburban area. Atmos. Environ. 40, 1134–1147.
Plaza, J., Artíñano, B., Salvador, P., Gómez-Moreno, F.J., Pujadas, M., Pio, C.A., 2011. Short-term secondary organic carbon estimations with a modified OC/EC primary ratio method at a suburban site in Madrid (Spain). Atmos. Environ. 45, 2496–2506.
Putaud, J.P., Van Dingenen, R., Alastuey, A., Bauer, H., Birmili, W., Cyrys, J., Flentje, H., Fuzzi, S., Gehrig, R., Hansson, H.C., Harrison, R.M., Herrmann, H., Hitzenberger, R., Hüglin, C., Jones, A.M., Kasper-Giebl, A., Kiss, G., Kousa, A., Kuhlbusch, T.a.J., Löschau, G., Maenhaut, W., Molnar, A., Moreno, T., Pekkanen, J., Perrino, C., Pitz, M., Puxbaum, H., Querol, X., Rodriguez, S., Salma, I., Schwarz, J., Smolik, J., Schneider, J., Spindler, G., Ten Brink, H., Tursic, J., Viana, M., Wiedensohler, A., Raes, F., 2010. A European aerosol phenomenology—3: physical and chemical characteristics of particulate matter from 60 rural, urban, and kerbside sites across Europe. Atmos. Environ. 44, 1308–1320.
Querol, X., Alastuey, A., Moreno, T., Viana, M.M., Castillo, S., Pey, J., Rodríguez, S., Artiñano, B., Salvador, P., Sánchez, M., Garcia Dos Santos, S., Herce Garraleta, M.D., Fernandez-Patier, R., Moreno-Grau, S., Negral, L., Minguillón, M.C., Monfort, E., Sanz, M.J., Palomo-Marín, R., Pinilla-Gil, E., Cuevas, E., De La Rosa, J., Sánchez De La Campa, A., 2008. Spatial and temporal variations in airborne particulate matter (PM_{10} and $PM_{2.5}$) across Spain 1999–2005. Atmos. Environ. 42, 3964–3979.
Salma, I., Ocskay, R., Raes, N., Maenhaut, W., 2005. Fine structure of mass size distributions in an urban environment. Atmos. Environ. 39, 5363–5374.
Salvador, P., Artíñano, B., Alonso, D.G., Querol, X., Alastuey, A., 2004. Identification and characterisation of sources of PM_{10} in Madrid (Spain) by statistical methods. Atmos. Environ. 38, 435–447.
Salvador, P., Artíñano, B., Viana, M., Alastuey, A., Querol, X., 2012. Evaluation of the changes in the Madrid metropolitan area influencing air quality: analysis of 1999–2008 temporal trend of particulate matter. Atmos. Environ. 57, 175–185.
Salvador, P., Artíñano, B., Molero, F., Viana, M., Pey, J., Alastuey, A., Querol, X., 2013. African dust contribution to ambient aerosol levels across central Spain: characterization of long-range transport episodes of desert dust. Atmos. Res. 127, 117–129.
Schleicher, N.J., Norra, S., Chai, F., Chen, Y., Wang, S., Cen, K., Yu, Y., Stüben, D., 2011. Temporal variability of trace metal mobility of urban particulate matter from Beijing—a contribution to health impact assessments of aerosols. Atmos. Environ. 45, 7248–7265.
Schmid, H., Laskus, L., Jürgen Abraham, H., Baltensperger, U., Lavanchy, V., Bizjak, M., Burba, P., Cachier, H., Crow, D., Chow, J., Gnauk, T., Even, A., Ten Brink, H.M., Giesen, K.-P., Hitzenberger, R., Hueglin, C., Maenhaut, W., Pio, C., Carvalho, A., Putaud, J.-P., Toom-Sauntry, D., Puxbaum, H., 2001. Results of the "carbon conference" international aerosol carbon round robin test stage I. Atmos. Environ. 35, 2111–2121.

Schwarz, J., Chi, X., Maenhaut, W., Civiš, M., Hovorka, J., Smolík, J., 2008. Elemental and organic carbon in atmospheric aerosols at downtown and suburban sites in Prague. Atmos. Res. 90, 287–302.

Seinfeld, J.H., Pandis, S.N., 1998. Atmospheric chemistry and physics—from air pollution to climate change. John Wiley & Sons, Inc., New Jersey, USA.

Sillanpaa, M., Frey, A., Hillamo, R., Pennanen, A.S., Salonen, R.O., 2005. Organic, elemental and inorganic carbon in particulate matter of six urban environments in Europe. Atmos. Chem. Phys. 5, 2869–2879.

Subramanian, R., Donahue, N.M., Bernardo-Bricker, A., Rogge, W.F., Robinson, A.L., 2007. Insights into the primary–secondary and regional–local contributions to organic aerosol and $PM_{2.5}$ mass in Pittsburgh, Pennsylvania. Atmos. Environ. 41, 7414–7433.

Terzi, E., Argyropoulos, G., Bougatioti, A., Mihalopoulos, N., Nikolaou, K., Samara, C., 2010. Chemical composition and mass closure of ambient PM10 at urban sites. Atmos. Environ. 44, 2231–2239.

Turpin, B.J., Huntzicker, J.J., 1995. Identification of secondary organic aerosol episodes and quantitation of primary and secondary organic aerosol concentrations during SCAQS. Atmos. Environ. 29, 3527–3544.

Viana, M., Chi, X., Maenhaut, W., Querol, X., Alastuey, A., Mikuška, P., Večeřa, Z., 2006. Organic and elemental carbon concentrations in carbonaceous aerosols during summer and winter sampling campaigns in Barcelona, Spain. Atmos. Environ. 40, 2180–2193.

Viana, M., Maenhaut, W., Chi, X., Querol, X., Alastuey, A., 2007. Comparative chemical mass closure of fine and coarse aerosols at two sites in south and west Europe: implications for EU air pollution policies. Atmos. Environ. 41, 315–326.

Vicente, A., Alves, C., Monteiro, C., Nunes, T., Mirante, F., Cerqueira, M., Calvo, A., Pio, C., 2012. Organic speciation of aerosols from wildfires in central Portugal during summer 2009. Atmos. Environ. 57, 186–196.

Viidanoja, J., Sillanpää, M., Laakia, J., Kerminen, V.-M., Hillano, R., Aarnio, P., Koskentali, T., 2002. Organic and black carbon in $PM_{2.5}$ and PM_{10}: 1 year of data from an urban site in Helsinki, Finland. Atmos. Environ. 36, 3183–3193.

Wall, S.M., John, W., Ondo, J.L., 1988. Measurement of aerosol size distributions for nitrate and major ionic species. Atmos. Environ. 22, 1649–1656.

Wang, Y., Zhuang, G., Sun, Y., An, Z., 2005. Water-soluble part of the aerosol in the dust storm season—evidence of the mixing between mineral and pollution aerosols. Atmos. Environ. 39, 7020–7029.

Wang, G., Kawamura, K., Xie, M., Hu, S., Gao, S., Cao, J., An, Z., Wang, Z., 2009. Size-distributions of n-alkanes, PAHs and hopanes and their sources in the urban, mountain and marine atmospheres over East Asia. Atmos. Chem. Phys. 9, 8869–8882.

Yuan, C.-S., Lee, C.-G., Liu, S.-H., Chang, J.-C., Yuan, C., Yang, H.-Y., 2006. Correlation of atmospheric visibility with chemical composition of Kaohsiung aerosols. Atmos. Res. 82, 663–679.

Zhang, X., Jiang, H., Jin, J., Xu, X., Zhang, Q., 2012. Analysis of acid rain patterns in northeastern China using a decision tree method. Atmos. Environ. 46, 590–596.